

Big Bang nucleosynthesis, matter–antimatter regions, extra relativistic species, and relic gravitational waves

Massimo Giovannini*

Institute of Theoretical Physics, University of Lausanne, BSP-1015 Dorigny, Switzerland

Hannu Kurki-Suonio[†] and Elina Keihänen[‡]

Department of Physical Sciences, University of Helsinki, P.O.Box 64, FIN-00014 University of Helsinki, Finland

(June 12, 2002)

Provided that matter–antimatter domains are present at the onset of big bang nucleosynthesis (BBN), the number of allowed additional relativistic species increases, compared to the standard scenario when matter–antimatter domains are absent. The extra relativistic species may take the form of massless fermions or even massless bosons, like relic gravitons. The number of additional degrees of freedom compatible with BBN depends, in this framework, upon the typical scale of the domains and the antimatter fraction. Since the presence of matter–antimatter domains allows a reduction of the neutron to proton ratio prior to the formation of ${}^4\text{He}$, large amounts of radiation-like energy density are allowed. Our results are compared with other constraints on the number of supplementary relativistic degrees of freedom and with different nonstandard BBN scenarios where the reduction of the neutron to proton ratio occurs via a different physical mechanism. The implications of our considerations for the upper limits on stochastic gravitational waves backgrounds of cosmological origin are outlined.

PACS numbers: 26.35.+c, 98.80.Ft, 98.80.Cq, 25.43.+t, 98.80.Es, 04.80.Nn, 04.30.-w

I. INTRODUCTION

The strongest constraint on additional energy density in the universe with a radiation-like equation of state is provided by big bang nucleosynthesis (BBN). The additional energy density speeds up the expansion and cooling of the universe, and, consequently, the typical time scale of BBN is reduced in comparison with the standard case. The additional radiation-like energy density may be attributed to some extra relativistic species whose statistics may be either bosonic or fermionic. Since the supplementary species may be fermionic, they have been customarily parametrized in terms of the effective number of neutrino species

$$N_{\text{eff}} = 3 + \Delta N_{\text{eff}}, \quad (1)$$

where $\Delta N_{\text{eff}} = 0$ corresponds to the standard case with no extra energy density. The standard BBN (SBBN) results are in agreement with the observed abundances for $N_{\text{eff}} = 2\text{--}4$, giving thus an upper limit $\Delta N_{\text{eff}} \lesssim 1$ [1–4].

Extra radiation-like energy can be also constrained by other physical considerations not directly related to BBN. However, the bounds seem to be much weaker than the ones provided by BBN. For instance, the growth of density perturbations in the early universe is affected by the radiation/matter energy density ratio, which in the standard case falls below unity some time before recombination. The data on CMB anisotropy [5] has now improved to the point where it can be used to provide a constraint [6–11]. Hannestad [6] obtains an upper bound $N_{\text{eff}} \lesssim 17$ (95% confidence), or $\Delta N_{\text{eff}} \lesssim 14$. Using

large scale structure (LSS) data in connection with the CMB data the same author also obtained a lower limit $N_{\text{eff}} \gtrsim 1.5/2.5$ (depending on the data set used).

The BBN and CMB limits are complementary. Both measure the increase in the expansion rate of the universe, but through completely different physical phenomena. They also look at different epochs in the history of the universe, BBN to $T = \mathcal{O}(1 \text{ MeV})$, CMB to $T = \mathcal{O}(1 \text{ eV})$. Thus attempts to relax one of these limits are unlikely to affect the other.

The BBN limits can be relaxed in nonstandard BBN (NSBBN) scenarios (see the extensive reviews [12] and [13], or [14]). For example, the ${}^4\text{He}$ yield can be affected by changing the electron neutrino spectrum, like in the model with active-sterile neutrino mixing [15], or by ν_e degeneracy, which changes the amount of thermal ν_e . This latter scenario is called degenerate BBN (DBBN) [16,17].

In the present paper yet a different scenario will be studied, namely BBN with matter–antimatter domains. In short the idea is the following. Consider the situation where matter–antimatter fluctuations [18,19], are present at the onset of BBN. The fluctuations will be described in terms of their typical scale and the relative amount of antimatter. In previous studies [20,21] it has been established that this type of scenario is rather effective in reducing the neutron to proton ratio prior to the formation of the ${}^4\text{He}$ abundance. The physical reason behind this statement is the different diffusion scale of protons and neutrons which can travel into antimatter domains annihilating there. Since the presence of extra relativistic species typically causes an increase in the neutron to proton ratio, it seems plausible that in the case of anti-

matter BBN (ABBN) more relativistic degrees of freedom can be accommodated than in the case of standard BBN scenarios.

The additional relativistic species may be also bosonic, for instance gravitons. This possible interpretation of the extra energy density at the BBN epoch was originally invoked by Schwartsman [22] since the production of gravitons is a generic phenomenon in Friedmann-Robertson-Walker (FRW) universes [23]. Relic gravitational waves decouple below the Planck scale and their energy density is constrained as part of the other extra relativistic species. The BBN bound constrains the maximal fraction of critical energy density present today in relic gravitons of cosmological origin. The experimental efforts are converging towards the possibility of direct detection of stochastically distributed gravitational waves [24,25]. Various resonant mass detectors are now operating at a typical frequency of the order of kHz (Allegro [26], Auriga [27], Explorer [28], Nautilus [29], Niobe [30]) and four Michelson interferometers (GEO-600 [31], TAMA-400 [32], LIGO [34] and VIRGO [33]) will soon be operating in a wide frequency band from a few Hz up to 10 kHz. It is interesting, in the context of ABBN, to elaborate on the possibility that the additional relativistic species are of gravitational origin.

The plan of our paper is the following. In Section II some basic considerations on BBN with extra relativistic species will be presented. In Section III the main features of ABBN will be summarized in light of the possible presence of additional relativistic degrees of freedom in the scenario. In Section IV the results of the analysis of the parameter space of ABBN will be reported. In Section V the findings of ABBN will be compared with the case of DBBN, while in Section VI the constraints on the additional relativistic species obtained in the framework of ABBN will be studied together with other constraints coming from different physical considerations. Section VII deals mainly with the implications of our results for the case of relic gravitational waves. Finally Section VIII contains our concluding remarks.

II. BBN WITH EXTRA ENERGY DENSITY

A. Preliminaries

In the radiation-dominated era the energy density of the universe is

$$\rho \equiv g_* \left(\frac{\pi^2}{30} \right) T^4. \quad (2)$$

This equation defines the effective number g_* of relativistic degrees of freedom [35]. An (ultra)relativistic fermion species with two internal degrees of freedom and in thermal equilibrium contributes $2 \cdot 7/8 = 7/4 = 1.75$ to g_* . Before neutrino decoupling the contributing relativistic

particles are photons, electrons, positrons, and $N_\nu = 3$ species of neutrinos, giving

$$g_* = \frac{11}{2} + \frac{7}{4}N_\nu = 10.75. \quad (3)$$

The neutrinos have decoupled before electron-positron annihilation so that they do not contribute to the entropy released in the annihilation. While they are relativistic, the neutrinos still retain an equilibrium energy distribution, but after the annihilation their temperature is lower, $T_\nu = (4/11)^{1/3}T$. Thus

$$g_* = 2 + \frac{7}{4}N_\nu \left(\frac{T_\nu}{T} \right)^4 = 2 + 0.454N_\nu = 3.36 \quad (4)$$

after electron-positron annihilation.

If we now assume that there are some additional relativistic degrees of freedom, which also have decoupled by the time of electron-positron annihilation, or just some additional component ρ_x to energy density with a radiation-like equation of state, $p_x = \rho_x/3$, its effect on the energy density and expansion rate of the universe is the same as that of having some (perhaps a fractional number of) additional neutrino species. Thus its contribution can be represented by replacing N_ν with $N_{\text{eff}} = N_\nu + \Delta N_{\text{eff}}$ in the above. Before electron-positron annihilation we have $\rho_x = (7/8)\Delta N_{\text{eff}}\rho_\gamma$ and after electron-positron annihilation we have $\rho_x = 0.227\Delta N_{\text{eff}}\rho_\gamma$.

The present ratio of the CMB ($T = 2.725$ K) energy density to the critical density is $\Omega_\gamma \equiv \rho_\gamma/\rho_c = 2.47 \times 10^{-5}h^{-2}$. If the extra energy density component has stayed radiation-like until today, its ratio to the critical density, Ω_x , is given by

$$h^2\Omega_x \equiv h^2\frac{\rho_x}{\rho_c} = 5.61 \times 10^{-6}\Delta N_{\text{eff}} \quad (5)$$

today*, where h is the Hubble constant in units of 100 km/s/Mpc.

* To be more precise, the neutrinos have not completely decoupled by the onset of electron-positron annihilation, so that some entropy does leak to the neutrino component. This effect, plus finite-temperature QED corrections, can be represented by using $N_{\text{eff}} = 3.04$ after e^\pm -annihilation in the $\Delta N_{\text{eff}} = 0$ case [36,37]. Mangano *et al.* [37] have considered the effect of extra relativistic species on this. Their numerical results (for $\Delta N_{\text{eff}} = 0-1$) can be approximated by $N_{\text{eff}} = 3.0395 + (1 - 0.0014)1.0074\Delta N_{\text{eff}}$ after e^\pm -annihilation, where the part $3.0395 - 0.0014 \times 1.0074\Delta N_{\text{eff}}$ is in neutrinos and $1.0074(1 - 0.00025\Delta N_{\text{eff}})\Delta N_{\text{eff}}$ is in the extra species [38]. This assumes that the extra energy density represented by ΔN_{eff} has completely decoupled before e^\pm annihilation. Here we have defined ΔN_{eff} as $N_{\text{eff}} - 3$ before e^\pm -annihilation, i.e., ΔN_{eff} is a constant parameter, whereas N_{eff} changes in the e^\pm annihilation. Then we have $\rho_x = 0.2288(1 - 0.00025\Delta N_{\text{eff}})\Delta N_{\text{eff}}\rho_\gamma$ after the e^\pm annihila-

B. Standard BBN and extra relativistic species

The BBN isotope most sensitive[†] to the expansion rate is ${}^4\text{He}$. The ${}^4\text{He}$ yield depends on the number of available neutrons, or on the number ratio n/p of neutrons and protons. This, in turn, is determined by the competition between the expansion rate and the rates of the weak reactions which convert neutrons into protons before the onset of the strong nuclear reactions which produce the isotopes. Extra energy density speeds up the expansion rate so that more neutrons remain available for ${}^4\text{He}$ production.

In the usual terminology, standard BBN (SBBN) has $\Delta N_{\text{eff}} = 0$, or $N_{\text{eff}} = N_\nu = 3$. Then SBBN is a one-parameter theory, with the present baryon-to-photon ratio

$$\eta \equiv 10^{10} \eta_{10} \equiv \frac{n_b}{n_\gamma} \quad (6)$$

the only free parameter. It is related to Ω_b , the fraction of critical density in baryonic matter today, by

$$\Omega_b h^2 = 3.65 \times 10^{-3} \eta_{10}. \quad (7)$$

For the purpose of the present discussion we expand the concept of SBBN by allowing the presence of extra radiation-like energy density, so that SBBN has two parameters, η and N_{eff} .

Since Y_p , the primordial ${}^4\text{He}$ mass fraction, is an increasing function of both N_{eff} and η in SBBN, the effect of a larger N_{eff} can be compensated by a *lower* η to keep Y_p in the observed range.

The effect of the expansion rate on the other isotopes, D, ${}^3\text{He}$, and ${}^7\text{Li}$ can be divided into two parts:

1. The higher n/p ratio leads to an increase in the yield of the other isotopes too.
2. The yields of these other isotopes are also sensitive to the time scale while these isotopes are produced by the strong nuclear reactions. The effect of less time can be compensated by increasing the reaction rates by increasing the baryon density.

These effects work in the same direction for D and for ${}^3\text{He}$, but (for $\eta_{10} \gtrsim 3$) in the opposite direction for ${}^7\text{Li}$, for which the second effect is stronger. Thus the net

tion and $\Omega_x = (1 - 0.00025 \Delta N_{\text{eff}}) 5.653 \times 10^{-6} h^{-2} \Delta N_{\text{eff}}$ today. Since antimatter annihilation effects in our ABBN scenario take place in part during the same period as e^\pm -annihilation, the quantity ΔN_{eff} constrained by our calculations is intermediate between ΔN_{eff} and $N_{\text{eff}} - 3$ after e^\pm -annihilation. We ignore these small effects in the present work.

[†]The magnitude of the effect on an isotope is considered in terms of how accurately its primordial abundance can be determined from observations.

effect on the other isotopes is to shift the agreement with observations towards *higher* η . This soon leads to conflict with Y_p , constraining ΔN_{eff} .

Copi, Schramm, and Olive [1] concluded that $N_{\text{eff}} < 4$ is a conservative upper limit. With various observational constraints on the primordial abundances, Lisi, Sarkar, and Villante [3] obtained 95% confidence limits in the range $N_{\text{eff}} = 2\text{--}4$. Using (probably prematurely) tight observational constraints, $\text{D}/\text{H} = 3.4 \pm 0.25 \times 10^{-5}$ and $Y_p = 0.244 \pm 0.002$, and the prior $N_{\text{eff}} \geq 3.0$, Burles *et al.* [2] get a tight upper limit $N_{\text{eff}} < 3.20$ (95% confidence). Cyburt, Fields, and Olive [4] consider various fixed values of η (looking forward to the future precision determinations of η from the CMB anisotropy) and obtain the 95% confidence limits $N_{\text{eff}} \leq 3.6(3.0)$ for $\eta_{10} = 5.8$ and $N_{\text{eff}} \leq 4.1(3.9)$ for $\eta_{10} = 2.4$ with (without) the prior $N_{\text{eff}} \geq 3.0$.

To summarize, the obtained SBBN upper limits are

$$\Delta N_{\text{eff}} \leq 0.2 \dots 1.0 \quad (8)$$

depending on the observational constraints chosen. Translated into an upper limit to Ω_x they become

$$h^2 \Omega_x \leq 1.1 \dots 5.6 \times 10^{-6}. \quad (9)$$

III. BBN WITH MATTER–ANTIMATTER DOMAINS

BBN in the presence of antimatter regions has been discussed in [20,21]. In this scenario the baryon-to-photon ratio is not only inhomogeneous but also not positive definite. In spite of this the Universe is not matter–antimatter symmetric and the antimatter regions are small enough to be completely annihilated well before recombination, so that they escape the CMB spectral distortion bound [39]. This type of inhomogeneities can come from different baryogenesis scenarios [19].

The time when most of the annihilation takes place is determined by the size of the antimatter regions, and this, in its turn determines the nature of ABBN. Two different cases can be distinguished, depending on whether the annihilation takes place before or after ${}^4\text{He}$ is formed in nucleosynthesis. The relevant physics is completely different in the two cases.

The case of interest here is the one with the smaller distance scale, where the antimatter region is annihilated before significant amounts of ${}^4\text{He}$ is made. This corresponds to antimatter regions of typical radius r_A between 10^5 m and than 10^7 m. (We give all distances as comoving at $T = 1$ keV.) If the antimatter regions are even smaller they annihilate before neutrino decoupling and have no effect on BBN. The matter and antimatter are mixed by (anti)neutron diffusion. More neutrons than protons are annihilated and thus the n/p ratio is reduced compared to SBBN. Thus we get less ${}^4\text{He}$.

This reduction in Y_p due to neutron annihilation can be used to cancel the increase in Y_p due to a large ΔN_{eff} . Since both work by affecting the n/p ratio, the n/p part of the effect on the other isotopes is cancelled also, and one is left with the effect of the speed-up on the strong reactions. This shifts the agreement with observed abundances towards larger η for large ΔN_{eff} .

For calculations (see [21] for details), we assume an idealized geometry, where the antimatter regions are spherical with comoving radius r_A and have homogeneous antimatter density equal to the matter density outside the region. With this idealization, the ABBN scenario introduces two new parameters, r_A and R , where R is the antimatter/matter ratio in the universe. We assume $R < 1$ so that matter is left over after the antimatter regions have annihilated. Together r_A and R determine the number density of the antimatter regions (or the typical distance between neighboring antimatter regions).

In Fig. 1 we show the dependence of Y_p on r_A and R for $\eta_{10} = 6$ and $N_{\text{eff}} = 3$. We get the maximum effect for $r \sim 10^6$ – 10^7 m, when most of the annihilation takes place just before ${}^4\text{He}$ is made. For fixed r_A the effect is roughly proportional to R . For $r \lesssim 10^7$ m, the effect on the other isotopes is also via the n/p ratio and thus relatively small.

For $r > 10^7$ m, some of the annihilation takes place after ${}^4\text{He}$ formation, leading to significant production of ${}^3\text{He}$ and D. Because of ${}^3\text{He}$ overproduction, this region is not interesting for allowing larger N_{eff} .

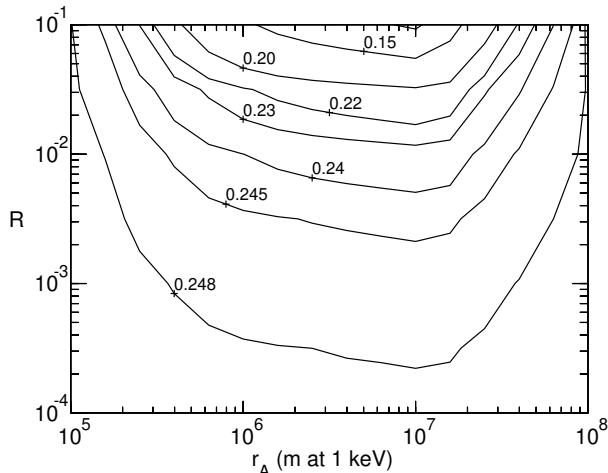


FIG. 1. The yield of ${}^4\text{He}$ as a function of the antimatter/matter ratio R and the radius r_A of the antimatter regions, for $\eta_{10} = 6.0$. The SBBN result, which is approached in the lower left corner, is $Y_p = 0.2484$.

IV. ABBN AND ADDITIONAL RELATIVISTIC SPECIES

The observational constraints on the primordial abundances of the light elements are a matter of some contro-

versy [40]. We follow Kneller *et al.* [9] in adopting the relatively generous constraints

$$0.23 \leq Y_p \leq 0.25 \quad (10)$$

$$2 \times 10^{-5} \leq \text{D}/\text{H} \leq 5 \times 10^{-5} \quad (11)$$

$$1 \times 10^{-10} \leq {}^7\text{Li}/\text{H} \leq 4 \times 10^{-10}. \quad (12)$$

We search for the region in the parameter space which satisfies these constraints. In SBBN these constraints lead to the upper limit $N_{\text{eff}} \leq 3.4$. For $N_{\text{eff}} = 3$ the same constraints limit η to the range $4.2 \leq \eta_{10} \leq 5.9$.

For $r_A < 10^7$ m, the effect of the antimatter regions on nucleosynthesis is mainly due to the reduction of the n/p ratio. As shown below, the dependence of the light element yields on r_A and R can be combined into a dependence on a single parameter, the n/p ratio at the onset of nucleosynthesis. This redundancy of parameters allows us to cover the whole phenomenology by varying three of the four parameters only. For most of our computations we kept the antimatter radius fixed at $r_A = 10^{6.9}$ m, in order to get the maximal reduction in n/p for a given value of R . This left us with three parameters η , N_{eff} , and R . We calculated the ABBN yields of light elements in this 3-dimensional parameter space and compared them to the observational constraints.

In Fig. 2 we show slices of this 3-dimensional parameter space for fixed values of η . For a given η , the upper limit on N_{eff} comes from a combination of the upper limit on D/H and the lower limit on ${}^4\text{He}$.

In Fig. 3 we show slices along another dimension, for fixed values of R . The allowed N_{eff} increases with increasing R . Simultaneously the allowed range in η shifts to higher values.

Fig. 4 illustrates the redundancy of parameters R and r_A . We show the yields of ${}^4\text{He}$ and deuterium as a function of r_A and R , for fixed $\eta_{10} = 6.0$ and $N_{\text{eff}} = 12$. The value of N_{eff} was chosen close to its upper limit for this value of η_{10} (see Fig. 2b). Reducing r_A moves the allowed region to higher values of R , but the width of the region remains nearly the same. Thus the effect of a smaller r_A can be compensated by a larger R . The contours of Y_p and D/H run almost parallel, so that we get essentially the same results for different combinations of r_A and R , which lie along these contours. This shows that the light element yields depend on a single function of R and r_A .

In Fig. 5 we show the projection of the allowed region in the $(\eta, N_{\text{eff}}, R)$ space onto the (η, N_{eff}) -plane. We see that very large amounts of extra radiation energy can be accommodated in ABBN. A large N_{eff} requires a somewhat larger η . For, e.g. $\eta_{10} = 6.0$ we obtain $3 \lesssim N_{\text{eff}} \lesssim 12.5$. Even values $N_{\text{eff}} > 20$ cannot be ruled out on the basis of nucleosynthesis. These large values require $\eta_{10} > 7$.

If we accept the possibility of ABBN, N_{eff} is no longer constrained by BBN, but is limited by other observational constraints.

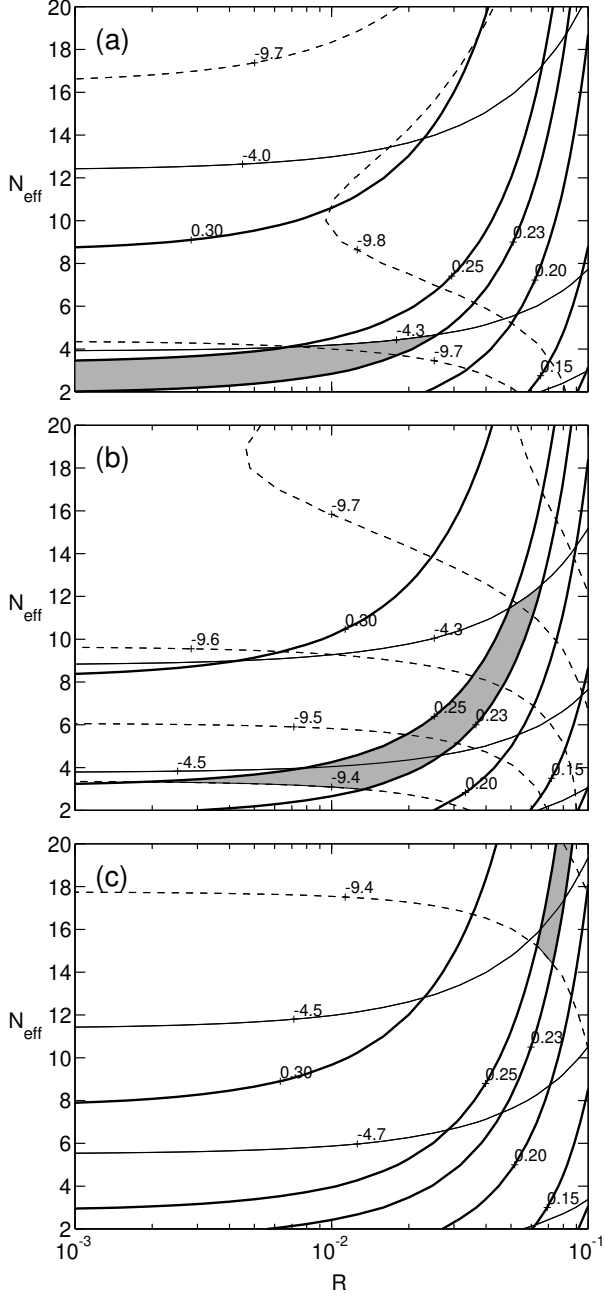


FIG. 2. The light element yields in ABBN for a fixed $r_A = 10^{6.9}$ m and $\eta_{10} = 4.5$ (a), 6.0 (b), and 9.0 (c), as a function of the two remaining parameters, R and N_{eff} . We show contours for Y_p (thick solid lines), $\log_{10} D/H$ (thin solid lines), and $\log_{10} {}^7\text{Li}/H$ (dashed lines). The shaded region is allowed by our adopted observational constraints.

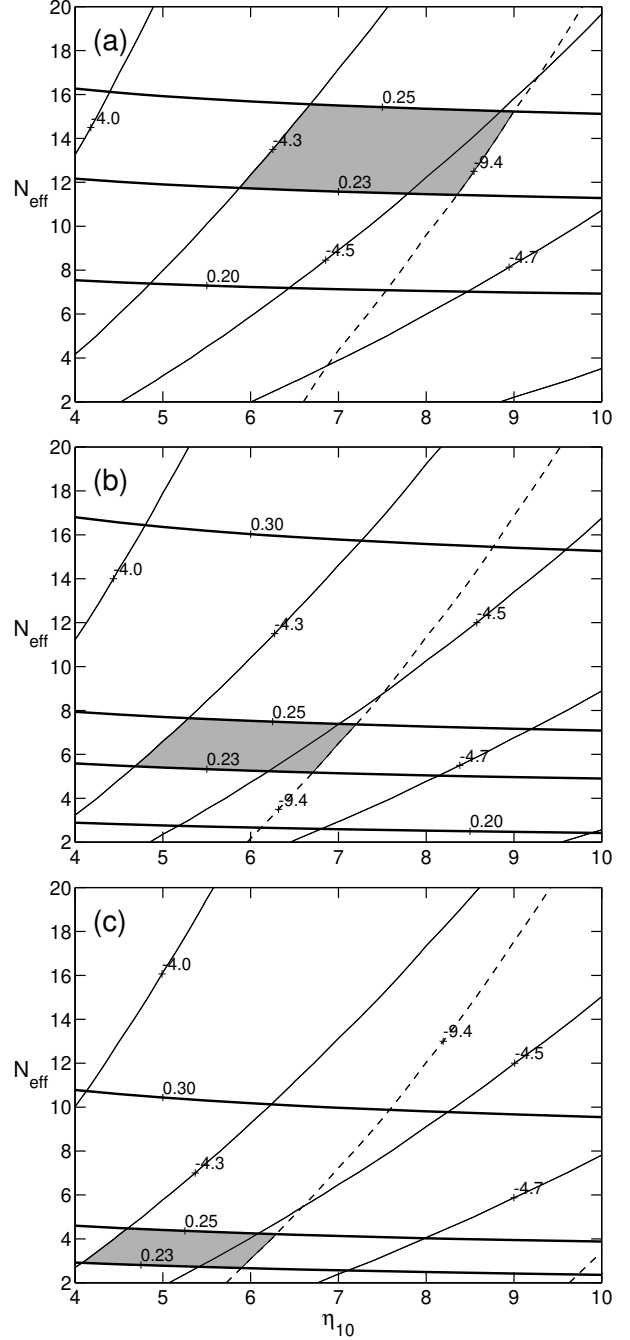


FIG. 3. The light element yields in ABBN for $r_A = 10^{6.9}$ m and antimatter/matter ratio $R = 10^{-1.2}$ (a), $10^{-1.5}$ (b), and 10^{-2} (c), as a function of η and N_{eff} . The line types and shading are the same as in Fig. 2.

V. COMPARING ABBN TO DBBN

A. Degenerate BBN

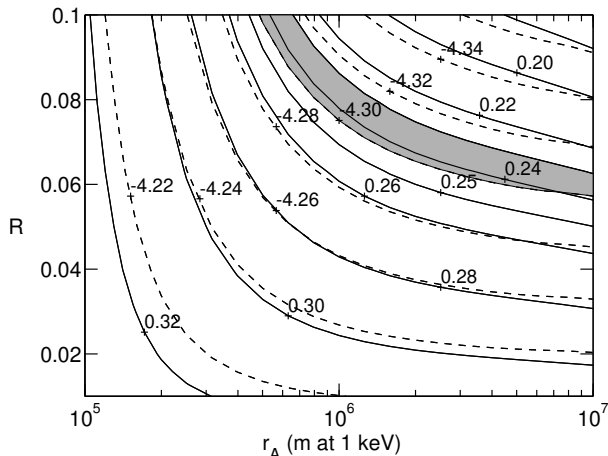


FIG. 4. The effect of the antimatter radius r_A on the production of ${}^4\text{He}$ and D. We show contours of Y_p (solid lines) and $\log_{10} D/H$ (dashed lines) on the (r_A, R) -plane, for $\eta_{10} = 6.0$ and $N_{\text{eff}} = 12$. The contours are almost parallel, showing that the yields depend on R and r_A only through a single combination.

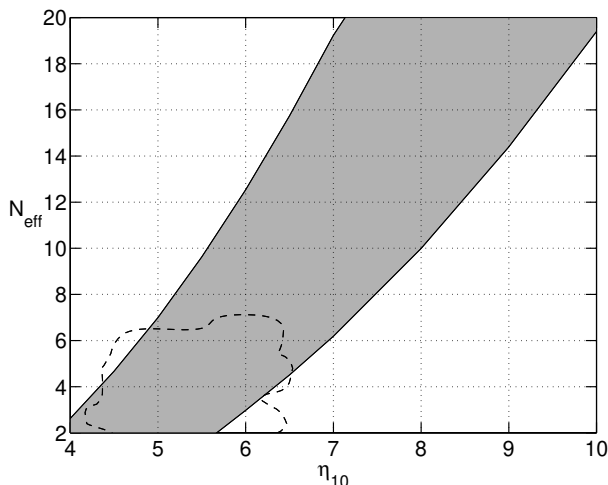


FIG. 5. The combined allowed region in (η, N_{eff}) . The shaded region indicates values of η, N_{eff} which are allowed for *some* value of the antimatter/matter ratio R . The dashed line is the CMB+SN Ia constraint from [10].

It is interesting to compare these results to another NS-BBN scenario, degenerate BBN (DBBN) [16,17], which is also very effective in reducing the ${}^4\text{He}$ yield. In SBBN the neutrino chemical potentials are assumed to be small, so that there are almost equal numbers of neutrinos and antineutrinos. In DBBN this assumption is lifted. The degeneracy parameters

$$\xi_i \equiv \frac{\mu_{\nu_i}}{T_\nu}, \quad (i = e, \mu, \tau), \quad (13)$$

stay constant as the temperature falls, as long as the neutrinos are relativistic. A nonzero ξ_i increases the energy density in neutrinos of type i by

$$\Delta N_{\text{eff}} = \frac{30}{7\pi^2} \xi_i^2 + \frac{15}{7\pi^4} \xi_i^4. \quad (14)$$

Degenerate neutrinos are thus one possibility for a nonzero (positive) ΔN_{eff} .

If the degeneracy is in electron neutrinos, a much stronger effect is that it shifts the balance of the weak reactions between neutrons and protons. The equilibrium ratio is

$$\left(\frac{n}{p}\right)_{\text{eq}} = e^{-Q/T - \xi_e}, \quad (15)$$

where $Q \equiv m_n - m_p$. Thus a positive ξ_e reduces n/p and thus Y_p , while a negative ξ_e increases n/p and Y_p . This effect is much larger than the speed-up effect from the ΔN_{eff} due to ξ_e . One can have both ΔN_{eff} and ξ_e as free parameters in this scenario by allowing the other ξ_i to have much larger (absolute) values than ξ_e (this possibility might, however, be excluded by neutrino oscillations [41]), or by assuming some other extra radiation-like energy density contribution.

In DBBN one can compensate the increase in Y_p due to a large ΔN_{eff} by a reduction due to a positive ξ_e . Like in ABBN, one then compensates for the speed-up effect on the other isotopes by increasing η . However this effect on these other isotopes is relatively small, and one can go to quite large ΔN_{eff} with a relatively small shift in η .

Considering BBN alone, the limit to ΔN_{eff} is practically removed. Combining DBBN limits with other cosmological bounds on the density and expansion rate of the universe, Kang and Steigman [17] obtained (in 1992) the limits $-0.06 \leq \xi_e \leq 1.1$, $|\xi_{\mu, \tau}| \leq 6.9$, which correspond to $\Delta N_{\text{eff}} \leq 71$, and $2.8 \leq \eta_{10} \leq 19$. The other cosmological constraints have since gotten tighter (see Sec. VI below).

B. ABBN versus DBBN

The DBBN allowed region in η and ΔN_{eff} (see, e.g., Fig. 2 of [8], Fig. 5 of [9], or Fig. 1 of [10]) is remarkably similar to that in ABBN (Fig. 5). We can understand this as follows.

In both cases the nonstandard feature affects nucleosynthesis mainly by reducing the n/p ratio, with practically arbitrarily large reductions possible. Thus the nonstandard parameters, (r, R) in the case of ABBN and ξ_e in the case of DBBN, can be mapped onto a reduction factor in n/p . The rest of the game is then the same: ΔN_{eff} can now be increased to bring the n/p ratio back up to give the observed value of Y_p ; this has then a small effect on the other isotopes by shortening the time available for nuclear reactions, which has to be compensated by an increase in η .

VI. DIFFERENT CONSTRAINTS ON ADDITIONAL RELATIVISTIC SPECIES

A large radiation energy density delays (i.e., moves to lower temperature) the transition from radiation domination to matter domination in the expansion law of the universe, and shortens the time scale of the radiation-dominated epoch. Since the radiation-dominated expansion law allows for logarithmic growth of density perturbations only, the large-scale structure of the universe constrains the radiation component. The effect of the radiation component in the expansion law shows also as an integrated Sachs-Wolfe (ISW) effect in the CMB angular power spectrum. Hannestad [6] used this to obtain an upper limit $N_{\text{eff}} < 17$ (95% confidence).

In connection with a NSBBN scenario one can go further and combine the NSBBN constraints on (η, N_{eff}) with the CMB constraints on (η, N_{eff}) . This has been done for DBBN in [7–10, 42]. These results will apply also to ABBN, since the allowed (η, N_{eff}) region is essentially the same in both NSBBN scenarios. This NSBBN allowed region leans towards higher η for high N_{eff} , whereas the CMB allowed region leans (slightly) towards lower η for high N_{eff} . The regions overlap for $\Delta N_{\text{eff}} \sim \text{few}$, but for the highest ΔN_{eff} allowed by CMB, the CMB seems to require a lower η than these NSBBN scenarios allow. Thus the combined constraint on ΔN_{eff} may be lower than that from CMB alone. Hansen *et al.* [10] use a different set of CMB data, favoring somewhat lower η , than Kneller *et al.* [9] use, and get therefore tighter combined upper limits for ΔN_{eff} .

Since the CMB spectrum depends on a large number of other cosmological parameters, these results are sensitive to the assumed priors on these other parameters. Kneller *et al.* [9] find that values of ΔN_{eff} larger than 10 are compatible with combined CMB and DBBN constraints, but when they include a prior on the matter density parameter, $\Omega_M \leq 0.4$, and on the age of the universe, $t \geq 11$ Gyr,

they get a tighter upper limit, $\Delta N_{\text{eff}} \lesssim 6$. Hansen *et al.* [10] get $\Delta N_{\text{eff}} \leq 5$ with a prior on the age, $t > 11$ Gyr, and $\Delta N_{\text{eff}} \leq 4$ (both at 95% CL) with a prior on the parameters Ω_M and Ω_Λ based on the supernova Ia data (see Fig. 5).

As emphasized by Hansen *et al.* [10], the determination of η from the CMB data relies on the heights of both the second and the third acoustic peaks in the CMB angular power spectrum, and, especially for the third peak, further data is needed to check on possible systematic effects. Therefore these combined CMB+NSBBN upper limits to ΔN_{eff} should be taken as preliminary.

At present, we can conclude that values of ΔN_{eff} as large as 4 are acceptable, and values somewhat larger, $\Delta N_{\text{eff}} = \mathcal{O}(10)$ may not yet have been ruled out. Thus, allowing for nonstandard BBN, like ABBN, raises the upper limit to the present fraction of extra radiation-like energy density from

$$h^2 \Omega_x \leq 1.1 \dots 5.6 \times 10^{-6} \quad (16)$$

to

$$h^2 \Omega_x \leq 2.3 \dots 8 \times 10^{-5}, \quad (17)$$

an increase by an order of magnitude.

VII. ABBN AND STOCHASTIC BACKGROUNDS OF RELIC GRAVITATIONAL WAVES

The supplementary radiation allowed either by ABBN or by DBBN may be the consequence of a primordial background of gravitational radiation. The present critical fraction of energy density stored in relic gravitons

$$h^2 \Omega_{\text{GW}}(t_0) \equiv h^2 \frac{\rho_{\text{GW}}}{\rho_c} = 5.6 \times 10^{-6} \Delta N_{\text{eff}}. \quad (18)$$

depends upon ΔN_{eff} whose range of variation can be translated into constraints on the energy density of relic gravitational waves produced prior to BBN. The critical fraction of spectral energy density per logarithmic interval of frequency

$$\Omega_{\text{GW}}(\nu, t_0) = \frac{1}{\rho_c} \frac{d\rho_{\text{GW}}}{d \ln \nu}. \quad (19)$$

is often introduced for practical purposes. Eqs. (8)–(9) (obtained in the context of SBBN) and Eqs. (16)–(17) (obtained in the context of ABBN) can then be interpreted, in light of Eq. (18), as an upper limit on the energy density presently stored in relic gravitons. Heeding experimental observations, the correlation of resonant mass detectors or of wide band interferometers can also provide upper bounds on the critical fraction of energy density stored in relic gravitons. The sensitivity of operating resonant mass detectors is not yet able to probe possible signals compatible with Eqs. (16)–(17)

and (18). Forthcoming generations of resonant mass and interferometric detectors are expected to improve their sensitivity in $h^2\Omega_{\text{GW}}$. The bounds coming from ABBN and from direct searches of stochastic gravitational wave backgrounds will represent two complementary sets of constraints on the same quantity.

A. GW detectors and BBN bound

Various resonant mass detectors are now operating [26–30]. In [43], the first experiment of cross-correlation between two cryogenic detectors has been reported with the purpose of giving an upper limit on $h^2\Omega_{\text{GW}}$. The two detectors are Explorer [28] (operating in CERN, Geneva) and Nautilus [29] (operating in Frascati, near Rome). Previous experiments giving upper limits on $h^2\Omega_{\text{GW}}$ used room temperature detectors. The Rome group obtained then an upper limit $h^2\Omega_{\text{GW}} < 60$ at a frequency of roughly 905 Hz. The limit is a result of cross-correlation between the two detectors (located at a distance of approximately 600 km) for an integration time of approximately 12 hours. This limit is not competitive with the BBN bound (and also above the critical density bound implying that $\Omega_{\text{GW}} < 1$). However, by increasing the correlation time from few hours to few months it is not unreasonable to go below one in $h^2\Omega_{\text{GW}}$.

Hollow spherical detectors have been recently investigated [44] as a possible tool for the analysis of the relic gravitational wave background. The sensitivity of two correlated spherical detectors could be $\mathcal{O}(10^{-6})$ in $h^2\Omega_{\text{GW}}$ for the frequency of resonance which lies between 200 and 400 Hz. In this case the ABBN bound and the experiment will be certainly competitive. Dual spherical detectors [45] may reach a sensitivity, in $h^2\Omega_{\text{GW}}$, which is again $\mathcal{O}(10^{-6})$ in the kHz region.

Consider now the case of wide band interferometers [31–34] whose arms range from 400 m of TAMA up to the 3 km of VIRGO and to the 4 km of LIGO. The foreseen noise power spectra $S_n(\nu)$ are defined for ν between a few Hz and 10 kHz. While at small frequency the seismic noise dominates, at higher frequencies the main source of noise is provided by the shot noise. The signal-to-noise ratio (SNR) will be obtained by comparing the analytic form of the noise power spectra with the possible stochastic signal parametrized in terms of $\Omega_{\text{GW}}(\nu)$. The single LIGO [34] detector will be presumably sensitive to $h^2\Omega_{\text{GW}} \sim 10^{-3}$. Two correlated interferometers lead to a SNR

$$\text{SNR}^2 = \frac{3H_0^2}{2\sqrt{2}\pi^2} F \sqrt{T} \times \left\{ \int_0^\infty d\nu \frac{\gamma^2(\nu) \Omega_{\text{GW}}(\nu)}{\nu^6 S_n^{(1)}(\nu) S_n^{(2)}(\nu)} \right\}^{1/2}, \quad (20)$$

(H_0 is the present value of the Hubble parameter and F depends upon the geometry of the two detectors; in

the case of the correlation between two interferometers $F = 2/5$). In Eq. (20), $S_n^{(k)}(\nu)$ is the (one-sided) noise power spectrum of the k -th ($k = 1, 2$) detector, while $\gamma(\nu)$ is the overlap reduction function [46–49] which is determined by the relative locations and orientations of the two detectors. This function cuts off (effectively) the integrand at a frequency $f \sim 1/2d$, where d is the separation between the two detectors. Eq. (20) assumes, as usually done, that the noises of the two detectors are stationary, Gaussian and not correlated.

Consider now the simple case of a flat spectrum, namely $\Omega_{\text{GW}}(\nu) = \Omega_0\nu^0$. From Eq. (20) using the appropriate expressions of the noise power spectra and of the overlap reduction functions pertaining to the LIGO and VIRGO detectors [50] we get that the sensitivity is

$$h^2\Omega_{\text{GW}} \simeq 1.8 \times 10^{-10} \left(\frac{1 \text{ yr}}{T} \right)^{1/2} \text{SNR}^2 \quad (21)$$

for the correlation between two LIGO detectors [49,50] and

$$h^2\Omega_{\text{GW}} \simeq 7.2 \times 10^{-8} \left(\frac{1 \text{ yr}}{T} \right)^{1/2} \text{SNR}^2 \quad (22)$$

for the hypothetical correlation of two VIRGO detectors [50]. In Eqs. (21) and (22) T is the integration time of, for instance, one year.

In the context of the standard BBN scenario we would be led to exclude $h^2\Omega_{\text{GW}} > 5.6 \times 10^{-6}$ as a signal of primordial origin. This bound can be relaxed, according to Eqs. (16)–(17) up to values which are $\mathcal{O}(10^{-4})$, in the context of ABBN. If a signal with $h^2\Omega_{\text{GW}}$ larger than the bound implied by standard BBN will ever be detected, it could still be of primordial nature. This observation may also be relevant for the bounds on stochastic GW backgrounds obtained by a single detector, where, $h^2\Omega_{\text{GW}}$ can be, at most $\mathcal{O}(10^{-4})$.

Microwave cavities have been originally proposed as GW detectors in the GHz–MHz region of the spectrum [51,52]. Their application for high frequency gravitational wave backgrounds was theoretically suggested in [53]. Improvements in the quality factors of the cavities (if compared with the prototypes of [51]) have been recently achieved [54] and two experiments (in Italy [54] and in England [55]) are now in progress. The sensitivity in $h^2\Omega_{\text{GW}}$ is still above one for the experiments reported so far. These devices could be important for the analysis of a frequency range where possible backgrounds generated by collections of astrophysical sources are negligible.

B. BBN bounds and theoretical models of stochastic GW backgrounds

When the ordinary inflationary phase (of de Sitter or quasi-de Sitter type) is followed by a radiation epoch gravitational waves are produced and the theoretically

estimated $\Omega_{\text{GW}}(\nu)$ decreases as ν^{-2} for $10^{-18} \text{ hHz} < \nu < 10^{-16} \text{ Hz}$. This branch of the spectrum corresponds to modes leaving the horizon during the inflationary phase and re-entering during the matter-dominated phase [56,57]. Since $\Omega_{\text{GW}}(\nu)$ is a decreasing function of the present frequency ν the most relevant bounds (determining the normalization of the spectrum) will be the ones coming from small frequencies (i.e. large length scales) and, among them, the analysis of the first thirty multipoles of temperature anisotropies in the microwave sky. The COBE normalization implies, in the low-frequency part of the inflationary spectrum, that $h^2\Omega_{\text{GW}}(\nu) < 6.9 \times 10^{-11}$ for $\nu \simeq 10^{-18} \text{ hHz}$.

The modes re-entering during the radiation dominated epoch correspond to frequencies $10^{-16} \text{ Hz} < \nu < 10^{-11} \sqrt{H_1/M_P} \text{ Hz}$, (where $H_1 \leq 10^{-6} M_P$ is the curvature scale at the end of inflation). The theoretical $\Omega_{\text{GW}}(\nu)$ is either a flat (exact Harrison-Zeldovich spectrum [58]) or a slightly decreasing (in the quasi-de Sitter case) function of ν , i.e. $\Omega_{\text{GW}}(\nu, t_0) \propto \nu^\alpha$, with $\alpha \leq 0$. Imposing the COBE normalization as illustrated above, it turns out that $\Omega_{\text{GW}}(\nu) < 10^{-15}$ for $\nu > 10^{-16} \text{ Hz}$. From Eqs. (21)–(22) and (18) it can be deduced that $\Omega_{\text{GW}} < 10^{-15}$ will always be compatible with the BBN constraints and out the foreseen sensitivity of wide band interferometers.

In quintessential inflationary models [59], the inflationary phase is not immediately followed by a radiation-dominated phase, but a long stiff phase (dominated by the kinetic energy of the quintessence field) takes place prior to the dominance of radiation. As a consequence, $\Omega_{\text{GW}}(\nu)$ increases as ν (up to logarithmic corrections) for $10^{-3} \text{ Hz} < \nu < \text{GHz}$ [60]. This branch of the spectrum corresponds to modes leaving the horizon during the inflationary phase and re-entering during the stiff phase. Around the GHz, $h^2\Omega_{\text{GW}}(\nu)$ exhibits a spike. While the presence of the spike is a consequence of the fact that the inflationary epoch is followed by a stiff phase, the height of the spike is bounded by the BBN. In the case of standard BBN the height of the spike turns out to be, at most, 0.8×10^{-6} [60]. Using the ABBN constraint the height of the spike becomes 1.7×10^{-5} . In pre-big bang models a similar discussion applies since the spectra of relic gravitons increase with frequency [61] and the most significant phenomenological bounds will be the one provided by Eq. (18).

VIII. CONCLUSIONS

Big bang nucleosynthesis provides the tightest constraint on the radiation-like energy density in the universe. However, some nonstandard BBN scenarios remove this constraint. In particular, this is true for NSBBN scenarios which cause a large reduction of the neutron-to-proton ratio before ${}^4\text{He}$ is formed, such as ABBN and DBBN.

All nonstandard features, whose effect on BBN is entirely due to a reduction of n/p before the nuclei are produced, have the same effect on BBN constraints on ΔN_{eff} , provided a sufficiently large n/p reduction is possible. One can then consider just this n/p reduction as the nonstandard feature, and ignore the rest of the nonstandard physics as far as BBN is concerned.

The BBN upper limit to ΔN_{eff} is raised, since this n/p reduction can be cancelled by a corresponding n/p increase due to the shortening of the timescale caused by a positive ΔN_{eff} . This brings Y_p back to the observed value. A small effect on the other isotopes remains since the timescale for the nuclear reactions is also shortened by ΔN_{eff} . This can be compensated by an increase in η . Thus the larger ΔN_{eff} values require somewhat larger values of η . The required increase is about $\Delta\eta_{10} \sim \Delta N_{\text{eff}}/4$.

Allowing for nonstandard BBN removes the upper limit to additional energy density which comes from nucleosynthesis. Even when we include the other cosmological constraints, the limit is raised from $\Delta N_{\text{eff}} \sim 1$ at least to $\Delta N_{\text{eff}} \sim 4$, or from $h^2\Omega_x = \text{few} \times 10^{-6}$ to $h^2\Omega_x = \text{few} \times 10^{-5}$. Even values up to $h^2\Omega_x = 8 \times 10^{-5}$ may be acceptable. Since, after BBN, gravitational waves interact very weakly with the surrounding plasma, the upper limit of BBN sets, today, an upper limit on the critical fraction of energy density stored in gravitational waves of primordial origin. In the near future various detectors will be able to reach sensitivities, in $h^2\Omega_{\text{GW}}$, which could be $\mathcal{O}(10^{-5})$ or even smaller. Hence, the problem will be to understand whether the obtained signal is primordial or not. The bound on extra relativistic species obtained in the context of ABBN may be then relevant since $h^2\Omega_{\text{GW}}$ cannot certainly be larger than 10^{-4} but it can be larger than $\sim 5 \times 10^{-6}$, constraint of the standard BBN scenario. If a signal compatible with $h^2\Omega_{\text{GW}} > 5.6 \times 10^{-6}$ will ever be found (either by two correlated resonant mass detectors or, most probably, by two correlated Michelson interferometers), it could still be of primordial origin provided $h^2\Omega_{\text{GW}} < \mathcal{O}(10^{-4})$.

IX. ACKNOWLEDGMENTS

We thank the Center for Scientific Computing (Finland) for computational resources. On behalf of the ROG collaboration we thank V. Fafone and G. Pizzella, for important discussions. Stimulating comments from E. Picasso, G. Gemme, and D. Babusci are also acknowledged. We thank S. Pastor, K. Abazajian, and S. Hansen for useful comments, S. Pastor for additional details concerning the results in Ref. [37] and S. Hansen for the CMB+SN Ia contour in Fig. 5.

- * Electronic address: massimo.giovannini@ipt.unil.ch
† Electronic address: hannu.kurki-suonio@helsinki.fi
‡ Electronic address: elina.keihanen@helsinki.fi
- [1] C.J. Copi, D.N. Schramm, and M.S. Turner, *Phys. Rev. D* **55**, 3389 (1997).
 - [2] S. Burles, K.M. Nollett, J.W. Truran, and M.S. Turner, *Phys. Rev. Lett.* **82**, 4176 (1999).
 - [3] E. Lisi, S. Sarkar, and F.L. Villante, *Phys. Rev. D* **59**, 123520 (1999).
 - [4] R. Cyburt, B. Fields, and K. Olive, *Astropart. Phys.* **17**, 87 (2002).
 - [5] C.B. Netterfield *et al.*, astro-ph/0104460; P. de Bernardis *et al.*, *Astrophys. J.* **564**, 559 (2002) A.T. Lee *et al.*, *Astrophys. J. Lett.* **561**, L1 (2001); R. Stompor *et al.*, *ibid.* **561**, L7 (2001); N.W. Halverson *et al.*, *Astrophys. J.* **568**, 38 (2002); C. Pryke, N.W. Halverson, E.M. Leitch, J. Kovac, J.E. Carlstrom, W.L. Holzapfel, and M. Dragan, *ibid.* **568**, 46 (2002); S. Padin *et al.*, *Astrophys. J. Lett.* **549**, L1 (2001).
 - [6] S. Hannestad, *Phys. Rev. Lett.* **85**, 4203 (2000); *Phys. Rev. D* **64**, 083002 (2001).
 - [7] M. Orito, T. Kajino, G.J. Mathews, and R.N. Boyd, astro-ph/0005446.
 - [8] S. Esposito, G. Mangano, A. Melchiorri, G. Miele, and O. Pisanti, *Phys. Rev. D* **63**, 043004 (2001).
 - [9] J.P. Kneller, R.J. Scherrer, G. Steigman, and T.P. Walker, *Phys. Rev. D* **64**, 123506 (2001)
 - [10] S.H. Hansen, G. Mangano, A. Melchiorri, G. Miele, and O. Pisanti, *Phys. Rev. D* **65**, 023511 (2002).
 - [11] R. Bowen, S.H. Hansen, A. Melchiorri, J. Silk, and R. Trotta, astro-ph/0110636.
 - [12] R.A. Malaney and G.J. Mathews, *Phys. Rep.* **229**, 145 (1993).
 - [13] S. Sarkar, *Rep. Prog. Phys.* **59**, 1493 (1996).
 - [14] H. Kurki-Suonio, astro-ph/0002071.
 - [15] See, e.g., R. Foot, M.J. Thomson, and R.R. Volkas, *Phys. Rev. D* **53**, 5349 (1996); X. Shi, G.M. Fuller, and K. Abazajian, *Phys. Rev. D* **60**, 063002 (1999); K. Enqvist, K. Kainulainen, and A. Sorri, *Phys. Lett.* **B464**, 199 (1999); *JHEP* **0104**, 012 (2001); P. Di Bari and R. Foot, *Phys. Rev. D* **63**, 043008 (2001).
 - [16] R.V. Wagoner, W.A. Fowler, and F. Hoyle, *Astrophys. J.* **148**, 3 (1967); A. Yahil and G. Beaudet, *ibid.* **206**, 26 (1976); Y. David and H. Reeves, *Philos. Trans. R. Soc. London* **A296**, 415 (1980); R.J. Scherrer, *Mon. Not. R. Astron. Soc.* **205**, 683 (1983); N. Terasawa and K. Sato, *Astrophys. J.* **294**, 9 (1985); K.A. Olive, D.N. Schramm, D. Thomas, and T.P. Walker, *Phys. Lett.* **B265**, 239 (1991); K. Kohri, M. Kawasaki, and K. Sato, *Astrophys. J.* **490**, 72 (1997).
 - [17] H.-S. Kang and G. Steigman, *Nucl. Phys.* **B372**, 494 (1992).
 - [18] R.W. Brown and F.W. Stecker, *Phys. Rev. Lett.* **43**, 315 (1979); G. Senjanović and F.W. Stecker, *Phys. Lett.* **96B**, 285 (1980); V.A. Kuzmin, M.E. Shaposhnikov, and I.I. Tkachev, *ibid.* **105B**, 167 (1981); A.K. Mohanty and F.W. Stecker, *ibid.* **143B**, 351 (1984); F.W. Stecker, *Nucl. Phys.* **B252**, 25 (1985).
 - [19] D. Comelli, M. Pietroni, and A. Riotto, *Nucl. Phys.* **B412**, 441 (1994); G.M. Fuller, K. Jedamzik, G.J. Mathews, and A. Olinto, *Phys. Lett.* **B333**, 135 (1994); M. Giovannini and M.E. Shaposhnikov, *Phys. Rev. Lett.* **80**, 22 (1998); *Phys. Rev. D* **57**, 2186 (1998); A.D. Dolgov, *Phys. Rep.* **222**, 309 (1992); hep-ph/9605280; A. Dolgov and J. Silk, *Phys. Rev. D* **47**, 4244 (1993); M.Yu. Khlopov, S.G. Rubin, and A.S. Sakharov, *Phys. Rev. D* **62**, 083505 (2000); M.Yu. Khlopov, R.V. Konoplich, R. Mignani, S.G. Rubin, and A.S. Sakharov, *Astropart. Phys.* **12**, 367 (2000).
 - [20] G. Steigman, *Ann. Rev. Astron. Astrophys.* **14**, 339 (1976); J.B. Rehm and K. Jedamzik, *Phys. Rev. Lett.* **81**, 3307 (1998); *Phys. Rev. D* **63**, 043509 (2001).
 - [21] H. Kurki-Suonio and E. Sihvola, *Phys. Rev. Lett.* **84**, 3756 (2000); *Phys. Rev. D* **62**, 103508 (2000); E. Sihvola, *Phys. Rev. D* **63**, 103001 (2001).
 - [22] V.F. Schwartzman, *Pis'ma Zh. Eksp. Teor. Fiz.* **9**, 315 (1969) [*JETP Lett.* **9**, 184 (1969)].
 - [23] L.P. Grishchuk, *Zh. Éksp. Teor. Fiz.* **67**, 832 (1974) [*Sov. Phys. JETP* **40**, 409 (1975)]; *Usp. Fiz. Nauk.* **156**, 297 (1988) [*Sov. Phys. Usp.* **31**, 940 (1988)].
 - [24] B.F. Schutz, *Class. Quant. Grav.* **16** A131 (1999).
 - [25] L.P. Grishchuk, V.M. Lipunov, K.A. Postnov, M.E. Prokhorov, B.S. Sathyaprakash, *Usp. Fiz. Nauk.* **171**, 3 (2001) [*Phys.Usp.* **44**, 1 (2001)].
 - [26] E. Mauceli *et al.*, *Phys. Rev. D* **54**, 1264 (1996).
 - [27] M. Cerdonio *et al.*, *Class. Quantum Grav.* **14**, 1491 (1997).
 - [28] P. Astone *et al.*, *Phys. Rev. D* **47**, 362 (1993).
 - [29] P. Astone *et al.*, *Astroparticle Physics*, **7**, 231 (1997).
 - [30] D.G. Blair *et al.*, *Phys. Rev. Lett.* **74**, 1908 (1995).
 - [31] K. Danzmann *et al.*, *Class. Quantum Grav.* **14**, 1471 (1997).
 - [32] K. Tsubono, *Gravitational Wave Experiments*, Proceedings of the E. Amaldi Conference, edited by E. Coccia, G. Pizzella, and F. Ronga (World Scientific, Singapore, 1995), p. 112.
 - [33] B. Caron *et al.*, *Class. Quantum Grav.* **14**, 1461 (1997).
 - [34] A. Abramovici *et al.*, *Science* **256**, 325 (1992).
 - [35] See, e.g., E.W. Kolb and M.S. Turner, *The Early Universe* (Addison-Wesley, Redwood City, California, 1990).
 - [36] D.A. Dicus, E.W. Kolb, A.M. Gleeson, E.C. Sudarshan, V.L. Teplitz, and M.S. Turner, *Phys. Rev. D* **26**, 2694 (1982); A.F. Heckler, *Phys. Rev. D* **49**, 611 (1994); A.D. Dolgov, S.H. Hansen, and D.V. Semikoz, *Nucl. Phys.* **B503**, 426 (1997); R.E. Lopez, S. Dodelson, A. Heckler, and M.S. Turner, *Phys. Rev. Lett.* **82**, 3952 (1999).
 - [37] G. Mangano, G. Miele, S. Pastor, and M. Peloso, *Phys. Lett.* **B534**, 8 (2002).
 - [38] S. Pastor, private communication.
 - [39] E.L. Wright *et al.*, *Astrophys. J.* **420**, 450 (1994); D.J. Fixsen, E.S. Cheng, J.M. Gales, J.C. Mather, R.A. Shafer, and E.L. Wright, *Astrophys. J.* **473**, 576 (1996).
 - [40] For reviews, see, e.g., D.N. Schramm and M.S. Turner, *Rev. Mod. Phys.* **70**, 303 (1998); K.A. Olive, in Particle Data Group, D. Groom *et al.*, *Eur. Phys. J.* **C15**, 133 (2000) (Review of Particle Physics); K.A. Olive, G. Steigman, and T.P. Walker, *Phys. Rep.* **333-334**, 389 (2000); D. Tytler, J.M. O'Meara, N. Suzuki, and D. Lubin, *Physica Scripta*, **T85**, 12 (2000), astro-ph/0001318.
 - [41] A.D. Dolgov, S.H. Hansen, S. Pastor, S.T. Petcov, G.G.

- Raffelt, and D.V. Semikoz, Nucl. Phys. **B632**, 363 (2002).
- [42] J. Lesgourgues and M. Peloso, Phys. Rev. D **62**, 081301 (2000); J. Lesgourgues and A.R. Liddle, Mon. Not. R. Astron. Soc. **327**, 1307 (2001).
- [43] P. Astone *et al.*, Astron. Astrophys. **351**, 811 (1999).
- [44] E. Coccia, V. Fafone, G. Frossati, J.A. Lobo, and J.A. Ortega, Phys. Rev. D **57**, 2051 (1998).
- [45] M. Cerdonio, L. Conti, J.A. Lobo, A. Ortolan, L. Tafarello, and J.P. Zendri, Phys. Rev. Lett. **87**, 031101 (2001).
- [46] P. Michelson, Mon. Not. R. Astron. Soc. **227**, 933 (1988).
- [47] N. Christensen, Phys. Rev. D **46**, 5250 (1992).
- [48] E.E. Flanagan, Phys. Rev. D **48**, 2389 (1993).
- [49] B. Allen and J.D. Romano, Phys. Rev. D **59**, 102001 (1999).
- [50] D. Babusci and M. Giovannini, Class. Quantum Grav. **17**, 2621 (2000); Phys. Rev. D **60**, 083511 (1999); Int. J. Mod. Phys. D **10**, 477 (2001).
- [51] F. Pegoraro, E. Picasso, and L.A. Radicati, J. Phys. A, **11**, 1949 (1978); F. Pegoraro, L.A. Radicati, Ph. Bernard, and E. Picasso, Phys. Lett. **68 A**, 165 (1978); E. Iacopini, E. Picasso, F. Pegoraro and L.A. Radicati, Phys. Lett. **73 A**, 140 (1979).
- [52] C.M. Caves, Phys. Lett. **80B**, 323 (1979); C.E. Reece, P.J. Reiner, and A.C. Melissinos, Nucl. Inst. and Methods, **A245**, 299 (1986); Phys. Lett. **104 A**, 341 (1984).
- [53] L.P. Grishchuk, Pis'ma Zh. Eksp. Teor. Fiz. **23**, 326 (1976).
- [54] Ph. Bernard, G. Gemme, R. Parodi, and E. Picasso, Rev. Sci. Instrum. **72**, 2428 (2001).
- [55] A.M. Cruise, Class. Quantum Grav. **17**, 2525 (2000); Mon. Not. R. Astron. Soc **204**, 485 (1983).
- [56] V.A. Rubakov, M.V. Sazhin, and A.V. Veryaskin, Phys. Lett. **115B**, 189 (1982).
- [57] R. Fabbri and M.D. Pollock, Phys. Lett. **125B**, 445 (1983); L.F. Abbott and M.B. Wise, Nucl. Phys. **224**, 541 (1984).
- [58] B. Allen, Phys. Rev. D **37**, 2078 (1988); V. Sahni, Phys. Rev. D **42**, 453 (1990); L.P. Grishchuk and M. Solokhin, Phys. Rev. D **43**, 2566 (1991); M. Gasperini and M. Giovannini, Phys. Lett. B **282**, 36 (1992).
- [59] P.J.E. Peebles and A. Vilenkin, Phys. Rev. D **59**, 063505 (1999).
- [60] M. Giovannini, Phys. Rev. D **60**, 123511 (1999); Class. Quantum Grav. **16**, 2905 (1999); Phys. Rev. D **58**, 083504 (1998).
- [61] M. Gasperini and M. Giovannini, Phys. Rev. D **47**, 1519 (1993); R. Brustein, M. Gasperini, M. Giovannini, and G. Veneziano, Phys. Lett. B **361**, 45 (1995).